



Published in final edited form as:

Nat Neurosci. 2009 October ; 12(10): 1238–1247. doi:10.1038/nn.2387.

SOX6 controls dorsal-ventral progenitor parcellation and interneuron diversity during neocortical development

Eiman Azim¹, Denis Jabaudon^{1,2}, Ryann Fame^{1,3}, and Jeffrey D. Macklis^{1,*}

¹MGH-HMS Center for Nervous System Repair, Departments of Neurosurgery and Neurology, Program in Neuroscience, Harvard Medical School; Nayef Al-Rodhan Laboratories, Massachusetts General Hospital; and Department of Stem Cell and Regenerative Biology, and Harvard Stem Cell Institute, Harvard University; Boston, Massachusetts 02114

³Department of Molecular and Cellular Biology, Harvard University, Cambridge, MA 02138

Summary

The extraordinary neuronal diversity of the central nervous system emerges largely from controlled spatial and temporal segregation of cell type-specific molecular regulators. Here, we report that the transcription factor SOX6 controls the molecular segregation of dorsal (pallial) from ventral (subpallial) telencephalic progenitors, and the differentiation of cortical interneurons, regulating forebrain progenitor and interneuron heterogeneity. During corticogenesis in mice, SOX6 and highly related SOX5 expression is largely mutually exclusive in pallial and subpallial progenitors, respectively, and remains mutually exclusive in a reverse pattern in postmitotic neuronal progeny. Loss of SOX6 from pallial progenitors causes their inappropriate expression of normally subpallium-restricted developmental controls, conferring mixed dorsal-ventral identity. In postmitotic cortical interneurons, loss of SOX6 dramatically disrupts the differentiation and diversity of cortical interneuron subtypes, analogous to SOX5 control over cortical projection neuron development. These data reveal SOX6 as a novel transcription factor regulator of both progenitor and cortical interneuron diversity during neocortical development.

Introduction

The two broad functional classes of cortical neurons, excitatory projection neurons and inhibitory interneurons, arise from spatially and molecularly-segregated pallial (dorsal) and subpallial (ventral) proliferative ventricular zones (VZ) of the telencephalon, respectively^{1,3}. Parcellation of these proliferative regions into molecularly segregated domains separated at the pallial-subpallial boundary (PSB) is critical for the generation of

Users may view, print, copy, and download text and data-mine the content in such documents, for the purposes of academic research, subject always to the full Conditions of use:http://www.nature.com/authors/editorial_policies/license.html#terms

*Correspondence: jeffrey_macklis@hms.harvard.edu.

²Current address: Department of Basic Neurosciences and Clinic of Neurology, University of Geneva, Switzerland

Author Contributions E.A. and J.D.M. designed the overall experimental directions and specific analyses, and wrote and edited the manuscript. E.A. also performed all experiments and data analysis. D.J. co-performed the microarray experiments, and assisted with interneuron quantification, microarray data evaluation, experimental design and data analysis, and manuscript writing and editing. R. F. performed whole mount *in situ* hybridization/immunocytochemistry, and assisted with BrdU/PH3 pallial progenitor analysis, microarray data evaluation, interneuron quantification, and manuscript editing. J.D.M. also contributed to data analysis and biological interpretation.

these distinct classes of neurons. Within these broad excitatory and inhibitory neuronal classes, tremendous subtype diversity arises largely from the dynamic temporal expression of progenitor and postmitotic transcriptional regulators. Both of these developmental mechanisms (inter- and intra-domain segregation of molecular regulators) combine to give rise to the extraordinary neuronal diversity of the adult mammalian brain.

The parcellation of the proliferative neuroepithelium at the PSB is defined and maintained by the interactions of several critical early patterning transcription factors, exemplified by the repressive interaction of pallium-expressed Neurogenin2 (Ngn2; also known as Neurog2) on the generally subpallium-expressed Mash1 (also known as Ascl1)¹. Accordingly, loss of Ngn2 function results in dorsal expansion of Mash1 expression, and a consequent ventralization of pallial progenitors, which aberrantly give rise to subpallial-like neurons^{4,5}. The dynamic interaction between this key pair of transcription factors exemplifies the delicate balance of molecular regulators in establishing and maintaining the PSB.

Throughout corticogenesis, these pallial and subpallial progenitors give rise to neurons, whose fate depends largely on the location and time at which they are born^{3,6-9}. In the pallium, excitatory projection neuron subtypes are born sequentially under the control of temporally-coordinated programs that guide their subtype specification and differentiation³. Simultaneously, inhibitory cortical interneurons, which constitute approximately 25% of all cortical neurons, are primarily born in the subpallial medial (MGE) and caudal ganglionic eminences (CGE)². Acquisition of distinct interneuron subtype identities, distinguishable by molecular, morphological, and electrophysiological phenotypes, depends on both the place and time of birth within the MGE and CGE^{2,6-12}. Differentiating interneurons then migrate tangentially toward and then radially into the cortex to populate their final laminar destinations alongside concurrently-born pallium-derived excitatory projection neurons^{2,13}. Since cortical interneurons are implicated in several developmental disorders¹⁴ including epilepsy¹⁵, autism¹⁶, and schizophrenia¹⁷, understanding the molecular controls over their subtype diversity might clarify some causes of and potential therapeutic approaches to these important disorders.

Though major progress has been made in elucidating regulation of broad aspects of neuronal heterogeneity during development¹, only recently have specific controls over excitatory^{3,18-26} and inhibitory²⁷⁻³¹ cortical neuron subtype differentiation been characterized. We recently reported that the transcription factor SOX5 postmitotically controls the sequential generation of distinct pallium-derived excitatory corticofugal projection neuron populations, regulating their subtype diversity^{22,26}. Motivated by the complementary and largely redundant functions of SOX5 and SOX6 in other systems^{32,33}, we hypothesized that SOX6 might also function in the generation of forebrain neuronal diversity.

SOX6 and SOX5 belong to the SRY-type HMG Box (SOX)-containing transcription factor family, composed of approximately 20 members in mammals, many of which have precise temporal and spatial function in cell fate specification and differentiation in multiple organ systems including the central nervous system^{34,35}. SOX6 and SOX5, which share 93%

identity in their HMG DNA-binding domains and 61% overall identity³⁶, interact and functionally overlap during chondrogenesis and oligodendroglial development in the spinal cord. During chondrogenesis, SOX6 and SOX5 are co-expressed in prechondrocytes, where they have overlapping and additive roles in promoting appropriate and timely differentiation into chondroblasts. Loss of either gene alone produces mild skeletal defects and perinatal death, while loss of both genes results in major cartilage dysgenesis and death during late gestation³². Similarly, SOX6 and SOX5 are co-expressed in developing oligodendroglia in the spinal cord, where they act as functionally equivalent repressors of specification and terminal differentiation³³. SOX6 has been reported to be expressed in the forebrain during mid-gestation by whole mount *in situ* hybridization³⁶ and in the early postnatal brain by Northern blot and RT-PCR³⁷, but without further investigation of cell-type specific expression or function.

Here, we report that in striking contrast to their overlapping expression and largely redundant functions in other systems, SOX6 and SOX5 are almost entirely mutually exclusively expressed in the forebrain, and have distinct, complementary functions. SOX6 and SOX5 exhibit complementary expression in pallial and subpallial progenitors, respectively, and this expression is remarkably reversed in differentiating postmitotic neurons, as progeny of subpallial progenitors (at least largely comprised of cortical interneurons) express SOX6, and corticofugal projection neuron progeny of pallial progenitors express SOX5. During development, SOX6 controls the segregation of pallial from subpallial progenitors by repressing the expression of Mash1 and downstream subpallium-specific programs in pallial progenitors. Postmitotically, SOX6 regulates multiple aspects of cortical interneuron differentiation, ultimately controlling the molecular diversity of cortical interneuron subtypes. We conclude that SOX6 and SOX5 play independent and complementary roles in the generation of neuronal diversity during neocortical development.

Results

SOX6 and SOX5 are mutually exclusively expressed

To determine whether SOX6 and SOX5 play complementary or interactive roles during neocortical development, we characterized their expression at key stages of corticogenesis. *In situ* hybridization and immunocytochemistry reveal that SOX6 and SOX5 are expressed in complementary and almost entirely mutually exclusive populations of progenitors and cortical neurons: SOX6 in pallial progenitors and postmitotic subpallial neurons, and SOX5 in subpallial progenitors and postmitotic pallial corticofugal projection neurons²² (Fig. 1a-e). Early in corticogenesis, SOX6 is expressed in the telencephalon in a slight dorsal-high to ventral-low gradient (Fig. 1b), while SOX5 is expressed in a spatially reciprocal ventral-high to dorsal-low gradient (Fig. 1c). During mid- to late corticogenesis, SOX6 and SOX5 have mutually exclusive expression in pallial (SOX6), and subpallial (SOX5) VZ progenitors (Fig. 1d,e and Supplementary Fig. 1). Their expression overlaps exclusively in a discrete portion of the dorsal subpallial VZ at the PSB (Supplementary Fig. 1b), a region that gives rise to the lateral cortical stream, populating basal telencephalic structures including the amygdala and piriform cortex^{38,39}.

Strikingly, the postmitotic progeny of pallial and subpallial progenitors mutually exclusively express SOX6 and SOX5 in a reverse pattern; SOX6 is expressed in the MGE and CGE mantle zones, which contain, among other neuronal populations, developing cortical interneurons that maintain SOX6 expression as they mature in the neocortex, while SOX5 is expressed by corticofugal projection neurons in the cortical plate²² (Fig. 1d,e and Supplementary Fig. 1a; also Fig. 6a). Notably, SOX6 is not expressed in the mantle zone of the LGE, where medium spiny neurons that populate the striatum will later mature (Fig. 1d). Immunocytochemical analysis of the S-phase marker BrdU, the pan-mitotic marker PCNA, and the M-phase marker phospho-histone 3 (PH3) reveals that subpallial expression of SOX6 is postmitotic (Supplementary Fig. 2) (though the theoretical possibility exists of low level, undetectable expression in mitotic cells). Taken together, these data indicate that SOX6 and SOX5 are expressed in spatially abutting, almost entirely non-overlapping populations of progenitors and postmitotic neurons, suggesting cross-repressive interactions during development.

SOX6 and SOX5 progenitor expression is cross-repressive

We hypothesized that if cross-repressive interactions exist, either direct or indirect, loss of either SOX6 or SOX5 would result in the corresponding ectopic expression of the other. Indeed, loss of SOX6 function in *Sox6* null (*Sox6*^{-/-}) mice³² results in expansion of SOX5 expression into the normally SOX6-expressing pallial VZ (Fig. 2a). During corticogenesis, this ectopic SOX5 expression gradually expands from the lateral to medial extent of the pallial VZ, suggesting a developmental gradient of SOX5 expression. Conversely, in *Sox5* null (*Sox5*^{-/-}) mice³², SOX6 expression expands ventrally into the subpallial VZ during neocortical development (Fig. 2b). This cross-repressive interaction is restricted to progenitors, and is not apparent in postmitotic neurons that express SOX6 or SOX5, indicating progenitor-specific, and possibly indirect, interactions between these two transcription factors, most likely in coordination with other progenitor patterning genes.

Remarkably, the dorsal subpallial VZ co-expresses SOX6 and SOX5 (Supplementary Fig. 1b), indicating a unique relationship in this distinct developmental domain, and suggesting that expression of either gene alone is not sufficient to repress the expression of the other. To investigate whether SOX6 and SOX5 are sufficient to repress expression of each other in progenitors, we mis-expressed SOX6 in the subpallial VZ and SOX5 in the pallial VZ via *in utero* electroporation at E12.5 for analysis at E16.5. Ectopic mis-expression of either gene revealed many transfected progenitors that continued to express the other (Supplementary Fig. 1c,d). This maintained co-expression after ectopic mis-expression of either gene is not surprising, given their normal co-expression in a discrete region of dorsal subpallial progenitors (Supplementary Fig. 1b), as well as in other developing systems^{32,33}, indicating that these two transcription factors can normally be co-expressed. Taken together, these data indicate that SOX6 and SOX5 are necessary, though not sufficient, to repress expression of each other in forebrain progenitors, strongly suggesting combinatorial interactions with other regional patterning signals during telencephalic development.

SOX6 and Ngn2 cooperatively control pallial identity

The complementary and mutually exclusive expression of SOX6 and SOX5 in forebrain progenitor domains is highly reminiscent of the generally non-overlapping expression of the critical patterning transcription factors Ngn2 (pallial) and Mash1 (subpallial)^{4,40}. Loss of Ngn2 causes ectopic expansion of Mash1 expression into pallial progenitors, activating downstream subpallial differentiation programs^{4,5}. Since the patterns of SOX6 and Ngn2 expression in telencephalic progenitors are largely superimposable, we examined whether loss of SOX6 function would result in a similar ventralization of the pallium. Indeed, loss of SOX6 causes a dramatic expansion of Mash1 expression into the pallial VZ throughout corticogenesis (Fig. 3a and Supplementary Fig. 3a). Interestingly, Olig2, a transcription factor also expressed by subpallial progenitors during corticogenesis, is also ectopically expressed in *Sox6*^{-/-} pallial VZ (Supplementary Fig. 3b). This domain-parcellating function is specific for SOX6, since loss of SOX5 function does not cause a reciprocal ventral expansion of pallium-specific Ngn2 expression, and simultaneous loss of both SOX6 and SOX5 function largely replicates the phenotype of *Sox6*^{-/-} mice (Supplementary Fig. 3c,d). These data indicate that SOX6 functions centrally in the molecular segregation of the pallial from the subpallial progenitor domain.

We next examined whether the partial ventralization of pallial progenitors in *Sox6*^{-/-} mice is due to disruption of the expression of mostly pallium restricted Pax6 or its direct downstream target Ngn2⁴¹. Pax6 (Supplementary Fig. 3e) and Ngn2 (Fig. 3b) are still normally expressed in the *Sox6*^{-/-} pallium, indicating that their expression is not centrally driven by SOX6. Since Ngn2 is known to normally repress Mash1⁴, and since this repression is lost in *Sox6*^{-/-} pallial progenitors (where Ngn2 and Mash1 are abnormally co-expressed), we hypothesized that SOX6 maintains pallial identity either (1) within and transcriptionally activated by the well described Pax6 → Ngn2 ⊣ Mash1 pathway, mediating Ngn2 repression of Mash1, or (2) in a previously undefined genetic cascade that does not require the Ngn2 pathway for transcriptional activation. To discriminate between these two possibilities, we examined the expression of SOX6 in the abnormally ventralized pallium of *Ngn2*^{-/-}/*Ngn1*^{-/-} mice⁴, in which the repression of Mash1 by Ngn2 (supplemented by additive repression by Ngn1) is lost⁴ (Fig 3c). Loss of SOX6 expression in the *Ngn2*^{-/-}/*Ngn1*^{-/-} pallium would suggest that SOX6 is a downstream transcriptional target of Ngn signaling, acting within this canonical pathway. The data exclude this alternative, since SOX6 expression is maintained in *Ngn2*^{-/-}/*Ngn1*^{-/-} pallium (Fig. 3d). Just as Ngn2 is normally expressed in the pallial VZ in the absence of SOX6, SOX6 is normally expressed in the absence of Ngn2. These data indicate that the cooperative convergence of both SOX6 and Ngn2 pathways is necessary to repress Mash1 and maintain the dorsal identity of pallial progenitors, while neither is sufficient on its own. In the absence of either of these critical regulators, pallial progenitors adopt a “blurred” dorsal-ventral identity, inappropriately co-expressing genes normally specific to one or the other developmental domain.

Despite the partial ventralization of *Sox6*^{-/-} pallial progenitors, projection neuron laminar distribution and subtype- and layer-specific molecular expression appears largely normal (Supplementary Fig. 4). Similarly, pallial progenitor proliferation is not affected by loss of SOX6 function, as assessed by BrdU uptake and PH3 expression (data not shown). In order

to determine whether the expansion of Mash1 expression into the *Sox6*^{-/-} pallium is indicative of the initiation of subpallium-specific programs of gene expression, we performed comparative microarray analysis between wildtype and *Sox6*^{-/-} pallium during mid-corticogenesis at E13.5, and identified several normally subpallium-specific genes ectopically expressed in the *Sox6*^{-/-} pallium, including *Dlx1*, *Dlx2*, *Dlx4*, *Gsh2*, *Isl1*, *Meis1*, as well as *Sox5* (Supplementary Table 1). These data indicate that SOX6 critically maintains pallial progenitor identity by repressing subpallial programs of gene expression, but critical redundant and/or compensatory controls (e.g. Ngn2 and Ngn1) persist that are sufficient to ensure largely appropriate pallial corticogenesis⁴².

Taken together, these results indicate that SOX6 controls the segregation of telencephalic progenitor domains during development, acting cooperatively with Ngn2 to repress subpallial identity in pallial progenitors.

SOX6 controls cortical interneuron subtype differentiation

SOX6 is also expressed in postmitotic interneurons as they reside in the subpallium and populate the neocortex (Fig. 1d and Supplementary Fig. 1a and 2 also Fig. 6a). We therefore examined whether loss of SOX6 function would affect sequential steps of interneuron differentiation, including (1) early postmitotic molecular identity; (2) cortical laminar location and morphology; and (3) interneuron molecular subtype differentiation. Our data indicate that SOX6 acts postmitotically, as cortical interneurons are born and differentiate, controlling their appropriate subtype development.

(1) Early postmitotic molecular identity—The early molecular programs of immature postmitotic cortical interneurons in the subpallial mantle zones largely determine and predict their appropriate differentiation⁴³. *Sox6*^{-/-} MGE and CGE mantle zones exhibit abnormal expression of Mash1 and Ngn2 (Fig. 3a,b), proneural transcription factors normally confined to VZ progenitors. SOX6 repression of the ectopic and persistent expression of normally progenitor and subpallium-specific Mash1, and normally progenitor and pallium-specific Ngn2, in subpallial mantle zones strongly suggests that SOX6 controls the temporal segregation of transcriptional programs between progenitors and postmitotic neurons.

Because MGE and CGE *Sox6*^{-/-} mantle zone cells ectopically Ngn2, which normally represses subpallial and maintains pallial identity⁴, we hypothesized that these cells might abnormally initiate pallium-like gene expression. Consistent with this hypothesis, *Sox6*^{-/-} subpallial mantle zone cells inappropriately express Vglut2, a vesicular glutamate transporter, whose expression is normally restricted to pallium-born excitatory projection neurons (Fig. 4a). This indicates that at least a subpopulation of *Sox6*^{-/-} subpallial immature neurons in the mantle zone are inappropriately differentiating.

In order to investigate whether this abnormal co-expression of pallial/subpallial and progenitor/postmitotic molecular regulators (Mash1, Ngn2, Vglut2) in *Sox6*^{-/-} immature subpallial neurons affects their ability to broadly differentiate into GABAergic neurons, we determined whether they express GAD67, (also known as Gad1), an enzyme necessary for the synthesis of the inhibitory neurotransmitter GABA, a fundamental indicator of their identity. Using *in situ* hybridization for *GAD67* (data not shown) and confirming using

GAD67-GFP (delta-neo) transgenic mice, in which GFP is expressed in the vast majority of GABA⁺ neurons^{28,44}, we find that in *Sox6*^{-/-};*GAD67-GFP* mice, GAD67 is expressed in neurons leaving the subpallial mantle zones (Fig. 4b), suggesting appropriate broad GABAergic neuron specification. However, as cortical interneurons continue their migration tangentially in one of two streams toward the cortex (a superficial marginal zone (MZ) stream or a deeper intermediate zone (IZ)/ subventricular zone (SVZ) stream), they seemingly fail to migrate properly in *Sox6*^{-/-} cortex, as indicated by the consistently less advanced leading edge of the MZ stream compared to the leading edge of the IZ/SVZ stream (Fig. 4b,c and Supplementary Fig. 5a). There is no change in the number of interneurons in either migratory stream at E13.5 (Fig. 4d and Supplementary Fig. 5b). From these data, we conclude that loss of SOX6 function perturbs the initial temporal segregation of progenitor-specific factors from postmitotic neurons, potentially causing their abnormal tangential migration, without affecting overall broad GABAergic neuron specification and abundance.

(2) Cortical laminar location and morphology—To further investigate whether the molecular and migratory irregularities in early stages of *Sox6*^{-/-} subpallial neuron differentiation are associated with abnormalities in subsequent stages of interneuron cortical invasion, we examined the laminar location and morphology of these interneurons as they populate the cortex. In *GAD67-GFP* mice at P0 (Fig. 5a), just after the interneurons have begun their radial migration into the maturing cortex, as well as at P14 (Fig. 5b), as they have more fully adopted their mature phenotypes, *Sox6*^{-/-} interneurons preferentially populate deeper neocortical layers (Fig. 5c,d), without any change in their total numbers. (Although the large majority of *Sox6*^{-/-} mice die perinatally, small numbers survive a few weeks postnatally, allowing P14 analysis³². *Sox6*^{+/-} mice survive to adulthood, though a small number exhibit occasional seizure behavior.) In examining the morphology of *GAD67-GFP*⁺ neurons at P0, in contrast to the mostly radial orientation of wildtype interneurons (reflecting their transition from tangential to radial migration), *Sox6*^{-/-} interneurons display abnormal, tangential orientation (Fig. 5a). These laminar distribution and morphological abnormalities are confirmed by analysis of the broad (at P0) interneuron marker calbindin (Calb) (Supplementary Fig. 6a). These data indicate that SOX6 plays a critical role in the differentiation of cortical interneurons as they integrate into the neocortical circuitry, manifested by their inappropriately deep laminar location and abnormal morphology.

(3) Interneuron molecular subtype differentiation—In order to determine whether SOX6 differentially affects the development of distinct cortical interneuron subtypes, we examined interneuron subpopulations using idiosyncratic molecular markers^{2,11}. By P14, the calcium-binding protein parvalbumin (PV) and the peptide hormone somatostatin (SST) are expressed by two non-overlapping subclasses of predominantly MGE-born interneurons, many of which are born early in corticogenesis; the peptide neurotransmitter neuropeptide Y (NPY) is expressed by normally later-born MGE and CGE-derived interneurons, many of which co-express SST; the peptide hormone vasoactive intestinal peptide (VIP) is predominantly expressed by late-born, CGE-derived interneurons, though a subpopulation of VIP⁺ interneurons co-express SST and might be of MGE origin; and the calcium-binding

protein calretinin (Calret) is predominantly expressed by late-born CGE interneurons, though a subpopulation also co-expresses SST and might be of MGE origin^{2,6,7,45,46}.

At P14, ~65% of all GAD67-GFP⁺ interneurons express SOX6, including: essentially all PV⁺ (86%) and SST⁺ (96%) interneurons (both the Calret⁺ (83%) and Calret⁻ (95%) subpopulations); over one-third of NPY⁺ interneurons (37%); essentially no VIP⁺ interneurons (3%); and only a small minority of Calret⁺ interneurons (11%) (Fig. 6a,b). Loss of SOX6 function results in a dramatic reduction in the number of interneurons expressing PV (93% reduction; $p < 0.0001$) and SST (70% reduction; $p = 0.002$), including the small population of SST⁺/Calret⁺ interneurons (79% reduction; $p = 0.03$), and the SST⁺/Calret⁻ interneurons (70% reduction; $p = 0.001$). Conversely, there is a corresponding dramatic increase in the number of NPY⁺ interneurons (137% increase; $p = 0.0009$), and no change in the number of VIP⁺ and Calret⁺ interneurons (Fig. 6c,d and Supplementary Fig. 6b-i). Notably, as observed with the general interneuron marker GAD67, all interneuron subtypes that normally express SOX6 inappropriately redistribute to deeper cortical layers in *Sox6*^{-/-} cortex (Supplementary Fig. 6c-i). At P0, when SST expression is normally seen in lateral neocortex and piriform cortex, there are already dramatically reduced numbers of *Sox6*^{-/-} SST⁺ interneurons (Supplementary Fig. 6b), indicating that SOX6 function is necessary from early stages of cortical interneuron molecular differentiation. Together, these data indicate that loss of SOX6 function causes a decrease in the abundance of particular molecularly-defined subtypes of cortical interneurons, many of which are normally MGE-derived during early corticogenesis, without affecting overall cortical interneuron number.

To investigate potential temporal control by SOX6 over cortical interneuron subtype differentiation, particularly given its preferential effects on largely early-born PV⁺ and SST⁺ MGE-derived interneurons^{2,6,7,45}, we performed dual birthdating of interneuron subtypes born at E11.5 and E15.5 using the halogenated thymidine analogues IdU and CldU, respectively⁴⁷, for examination at P14 (Fig. 7). In WT cortex, NPY⁺ interneurons are preferentially born during late versus early corticogenesis (~twice as many CldU⁺/NPY⁺ as IdU⁺/NPY⁺; 180%, $p = 0.02$) (Fig. 7a), confirming previous reports⁴⁶. Additionally, while the number of early- and late-born neurons are equivalent between WT and *Sox6*^{-/-} cortices, far fewer *Sox6*^{-/-} early- and late-born interneurons are PV⁺ and SST⁺ (early PV: 83% decrease; $p = 0.002$; early SST: 65% decrease; $p = 0.009$; late PV: 88% decrease; $p = 0.02$; late SST: 93% decrease; $p = 0.04$), while a dramatically increased number of early- and late-born cortical interneurons are NPY⁺ (early NPY: 40% increase; $p = 0.03$; late NPY: 90% increase; $p = 0.04$) (Fig. 7b). These data strongly suggest that, when SOX6 function is absent, many early- and late-born cortical interneurons that would normally differentiate into PV⁺ and/or SST⁺ subtypes inappropriately express NPY, which is normally preferentially expressed by later-born subtypes. Taken together, these data suggest that, much like the function of SOX5 in corticofugal projection neurons^{22,26}, SOX6 is necessary for appropriate cortical interneuron molecular subtype diversity, ensuring the appropriate temporal expression of subtype-defining and functionally central proteins.

Given the striking effects of loss of SOX6 function on the largely MGE-derived PV⁺ and SST⁺ interneurons without an effect on overall cortical interneuron numbers, we next examined whether loss of SOX6 function affects the expression of LHX6, a transcription

factor necessary for the appropriate development of MGE-derived cortical interneuron subtypes^{28,29}. In *Sox6*^{-/-} mice, LHX6 is expressed in MGE-born interneurons, but these neurons are disorganized as they segregate into migratory streams and populate the cortex at E13.5 (Fig. 8a), confirming the tangential migratory abnormalities observed in *Sox6*^{-/-};*GAD67-GFP* mice (Fig. 4b,c). These data indicate that SOX6 is required for appropriate subtype-specific differentiation from these earliest stages of interneuron development. At P14, after maturing interneurons have populated the cortex, while there is a modest drop in the abundance LHX6⁺ neurons in *Sox6*^{-/-} cortex (35% reduction; $p = 0.04$), most LHX6⁺ interneurons populate the cortex (Fig. 8b). Importantly, LHX6 is not ectopically expressed by neurons born from abnormally ventralized *Sox6*^{-/-} pallial progenitors (Fig. 8a) or in *Sox6*^{-/-} CGE (data not shown), indicating that, as in the normal brain, LHX6⁺ neurons in *Sox6*^{-/-} cortex are MGE-derived.

To determine whether the abnormally abundant NPY⁺ interneurons arise from the *Sox6*^{-/-} MGE population itself (“population autonomous” rather than due to changes outside of this population), we investigated whether there is an increase in the number of MGE-derived LHX6⁺ interneurons that express NPY in *Sox6*^{-/-} cortex. In WT cortex, very few LHX6⁺ neurons co-express NPY (1% \pm 0.5% of LHX6⁺ neurons), while *Sox6*^{-/-} cortex reveals a dramatic increase (23% \pm 3% of LHX6⁺ neurons) (~11.5-fold increase; $p = 0.004$) (Fig. 8c,d). Similarly, there is a very large increase in the number of NPY⁺ neurons that immunocytochemically co-label with LHX6 in *Sox6*^{-/-} cortex (22% \pm 3% of NPY⁺ neurons) as compared to WT (4% \pm 2% of NPY⁺ neurons). Additionally, the large majority of these *Sox6*^{-/-} LHX6⁺/NPY⁺ neurons are found in deep cortical layers (81% \pm 5%), further suggesting they are of early-born MGE origin (Fig. 8d). Taken together, these interneuron subtype analyses indicate that SOX6 functions in a population autonomous manner, controlling the appropriate molecular differentiation of MGE-derived cortical interneuron subtypes.

An additional (though not mutually exclusive) theoretical explanation for the increase in the number of *Sox6*^{-/-} NPY⁺ interneurons is that they might be born from abnormally ventralized *Sox6*^{-/-} pallial progenitors. However, the data indicate that *Sox6*^{-/-} NPY⁺ neurons are not pallium-derived: 1) LHX6⁺ interneurons in *Sox6*^{-/-} cortex do not express TBR1 (Supplementary Fig. 7a), a transcription factor broadly expressed by pallium-derived pyramidal neurons through P14; and 2) all NPY⁺ neurons in *Sox6*^{-/-} cortex express GAD67-GFP (Supplementary Fig. 7b), and GAD67-GFP is not expressed by neurons born from partially ventralized *Sox6*^{-/-} pallial progenitors (Fig. 4b).

Integrating our findings, we report that during telencephalic development, SOX6 is largely mutually exclusively expressed and cross-repressively interacts with highly related SOX5, critically controlling pallial progenitor identity and cortical interneuron differentiation and diversity. Interestingly, we previously demonstrated that subtype differentiation in the complementary population of corticofugal projection neurons is analogously controlled by SOX5²². Taken together, these simultaneous, independent, and functionally parallel postmitotic controls critically underlie much of the tremendous neuronal diversity in the neocortex (Supplementary Fig. 8).

Discussion

The extraordinary cellular diversity of the central nervous system arises largely from the parsimonious use of a relatively small number of genes across distinct cell types, exemplified here by the multiple and distinct functions of SOX6 during neocortical development. We show that the highly related transcription factors SOX6 and SOX5 (which are co-expressed with largely overlapping functions in other organ systems^{32,33}), are expressed and function in the telencephalon in a novel, cross-repressive, and complementary fashion. SOX6 functions cooperatively with previously described pallial/subpallial parcellation programs to control pallial progenitor identity, and it is critical for the subtype diversity of cortical interneurons, parallel to SOX5 function in pallium-derived corticofugal projection neurons²².

In the developing telencephalon, the repressive action of SOX6 and Ngn2⁴ on Mash1 expression is critical for maintaining pallial progenitor identity. Our data indicate 1) that the expression of SOX6 and Ngn2 are independent; 2) that these two Mash1 repressive interactions are cooperative; and 3) that both are individually necessary, though neither is on its own sufficient, for repressing subpallial identity. Interestingly, while Pax6 directly activates Ngn2 expression in the telencephalon, spinal cord, and retina⁴¹, it does not appear to act transcriptionally upstream or downstream of SOX6, since microarray analysis of *Pax6*^{-/-} pallium reveals no change in SOX6 expression⁴⁸, and the *Sox6*^{-/-} pallium exhibits no change in Pax6 expression. This strongly suggests that there are at least two pathways that restrict Mash1 expression to the subpallium: (1) a classic Pax6→Ngn2 pathway, and (2) a cooperative pathway in which SOX6 is expressed independently of Pax6 and Ngn2.

Despite dorsal ectopic expression of Mash1, SOX5, and other subpallial VZ signals in *Sox6*^{-/-} pallial progenitors, postmitotic projection neuron progeny appear to develop broadly normally. This contrasts with the apparently more severe ventralization of these neurons in *Ngn2*^{-/-} mice (e.g. extensive ectopic expression of GAD67)^{4,5}, suggesting that, although initial stages of ventralization occur in *Sox6*^{-/-} pallium (Supplementary Table 1), dorsal identity regulators that persist in *Sox6*^{-/-} pallial progenitors, including perhaps Ngn2 and Ngn1, are sufficient to override and mask Mash1 and other subpallial fate programs, as has been suggested⁴². Therefore SOX6 likely functions in concert with additional pallial patterning regulators to control dorsal identity.

Interestingly, SOX6 and SOX5 are co-expressed in a discrete region of the dorsal subpallial VZ near the PSB. This region encompasses a proliferative source for the lateral cortical stream, which populates structures of the basal limbic system including the amygdala and piriform cortex^{38,39}. These paleopallial structures are of older evolutionary origin than the neocortex of the neopallium. SOX6 and SOX5 may have been evolutionarily selected to act cooperatively in this unique population of progenitors, as they do in chondrocytes and spinal cord oligodendrocytes. In contrast, the later evolution of the neocortex may have driven the separation of these transcription factors, contributing to the evolution of mammalian neocortical development⁴⁹. Further molecular phylogenetic analysis might elucidate whether SOX6 and SOX5 cooperate during paleopallium development, and at what point SOX6 and SOX5 function diverged into discrete telencephalic progenitor and neuronal populations.

SOX6 is also necessary for successive stages of cortical interneuron postmitotic differentiation. Immature neurons in *Sox6*^{-/-} subpallial mantle zones exhibit “confused” progenitor/postmitotic and dorsal-ventral molecular identity, aberrantly expressing subpallial progenitor-restricted Mash1, pallial progenitor-restricted Ngn2, and pallial postmitotic-restricted Vglut2. As *Sox6*^{-/-} cortical interneurons mature, they are broadly correctly specified as GABAergic and populate the cortex in correct numbers, but finer molecular analysis reveals aberrant subtype differentiation, as exemplified by MGE-born cortical interneuron populations. In the absence of SOX6 function, there is a dramatic increase in the abundance of NPY⁺ interneurons at the expense of PV⁺ and SST⁺ interneurons, revealing abnormal subtype-defining neurotransmitter/molecular identity, one of multiple core contributing factors to the overall subtype identity and function of a neuron. Additional morphological and electrophysiological analyses might further examine whether these aberrant NPY⁺ interneurons fully adopt functions normally associated with NPY expression.

Three potential (and not mutually exclusive) processes might largely account for the dramatic loss of *Sox6*^{-/-} cortical interneuron molecular subtype diversity, without overall reduction of interneuron number. One possibility is that population autonomous subtype specification is primarily affected, such that MGE-derived interneurons that would normally differentiate into subtypes that express PV and/or SST abnormally differentiate and express the normally later-expressed NPY. Another possibility is that MGE-born interneurons that normally would have been PV⁺ and SST⁺ might selectively not populate the cortex, and CGE progenitors might simultaneously increase their NPY⁺ interneuron output. A third, similar possibility is that abnormally partially ventralized *Sox6*^{-/-} pallial progenitors are a source of these new NPY⁺ neurons, which populate the cortex in place of MGE-born interneurons.

Our data very strongly favor the first interpretation of population autonomous subtype differentiation, since 1) there is a very large increase in the number of MGE-derived LHX6⁺ interneurons that express NPY concomitant with their loss of PV and SST expression; 2) birthdating analysis reveals that, while the overall numbers of both early- and late-born neurons are unaffected by the loss of SOX6 function, a large number of early-born interneurons, which tend to arise from the MGE rather than the CGE, do not express PV or SST, but inappropriately express NPY; 3) abnormal molecular identity in the *Sox6*^{-/-} MGE mantle zone (Ngn2, Mash1, Vglut2), observed as soon as the interneurons are born, strongly suggests a population autonomous effect of SOX6 function very early in neuronal differentiation; 4) there is no evidence of a significant increase in the number of GAD67-GFP⁺ migrating interneurons originating from *Sox6*^{-/-} CGE, or any from the pallium, that would be required to compensate for the hypothetical loss of MGE-born interneurons (theoretically predicted for the second and third hypothetical possibilities outlined above); 5) specifically regarding the second possibility that the NPY⁺ neurons are all CGE-derived, it is neither likely, nor supported by any of the data, that *Sox6*^{-/-} CGE progenitor populations would increase their neurogenic rate in the absence of SOX6, since SOX6 is not normally even expressed in CGE VZ progenitors; and finally, 6) specifically regarding the third possibility that the NPY⁺ neurons are pallium-derived, in *Sox6*^{-/-} cortex, all NPY⁺ neurons

express GAD67, which the data show is not ectopically expressed in *Sox6*^{-/-} pallium-born neurons, and they do not express TBR1, a transcription factor broadly expressed by pallium-derived projection neurons, together strongly indicating that they are not born from pallial progenitors. Taken together, these results reinforce previous findings on the population-autonomous functions of SOX6 both within and outside of the nervous system^{32,33}, now revealing its function as a critical control over the appropriate molecular differentiation of MGE-derived cortical interneuron subtypes.

Additional interneuron developmental deficits might be occurring in the absence of SOX6 function. While all LHX6⁺ neurons in *Sox6*^{-/-} cortex express GAD67-GFP, indicating their broad differentiation into GABAergic interneurons, some do not express NPY, PV, SST, or other major cortical interneuron subtype molecular markers. This suggests that some *Sox6*^{-/-} MGE-derived interneurons might stall during later stages of subtype differentiation. Additionally, these data do not exclude the possibility that SOX6 also functions in the population autonomous subtype differentiation of SOX6⁺ CGE-derived cortical interneurons, or perhaps via additional non population-autonomous pathways.

NKX2-1 is a transcription factor that acts upstream of LHX6³⁰, and was recently shown to be critical for multiple stages of cortical interneuron development, including the temporal fate specification of cortical interneuron subtypes^{31,50}. Loss of NKX2-1 function results in a reduction in the number of PV⁺ and SST⁺ cortical interneurons, and a corresponding increase in the number of VIP⁺ and CR⁺ interneurons. Given the present findings, SOX6 might be functioning, at least partially, in the postmitotic downstream execution of NKX2-1 signaling, potentially cooperatively interacting with LHX6^{28,29}, thereby regulating the temporal pacing of MGE-derived cortical interneuron fate specification and differentiation (Supplementary Fig. 8). Additional gain- and loss-of-function analyses might elucidate potential functional interactions between these transcription factors during interneuron subtype specification and differentiation.

Much like pallium-born neuron subtypes, cortical interneuron subtype identity is largely determined by the time of birth. Fate mapping experiments using H³-thymidine labeling and, more recently, genetic tools investigating subtype specification within MGE-born interneurons, reveal that SST⁺ interneurons, which are strikingly diminished in number in *Sox6*^{-/-} cortex, are on average born at earlier stages of corticogenesis, while NPY⁺, VIP⁺, and CR⁺ interneurons, whose numbers are either increased or maintained in *Sox6*^{-/-} cortex, are born later^{7,31,45,46}. These data raise the hypothesis that, during cortical interneuron development, SOX6 participates in setting the pace for the proper timing of developmental transitions. In this model, loss of SOX6 might result in premature differentiation into neurons normally born at later developmental stages, at the expense of those born at early stages. Supporting this interpretation, dual IdU/CldU birthdating analysis of the molecular differentiation of early- and late-born neurons in *Sox6*^{-/-} cortex reveals that early-born neurons aberrantly differentiate and express the normally later-born subtype-defining protein NPY. As the lineage relationships of particular cortical interneuron subtypes are further clarified, it will be possible to discern whether loss of SOX6 function alters temporal development within a lineage (e.g. those that would normally be SST⁺ neurons aberrantly differentiate into NPY⁺ neurons born later potentially within the same lineage), and/or

whether lack of SOX6 function results in inappropriate differentiation across lineages (e.g. those that would normally be PV⁺ neurons aberrantly differentiate into NPY⁺ neurons born later from a potentially distinct lineage).

Intriguingly, we recently reported that loss of SOX5 function from pallium-derived corticofugal projection neurons results in the premature adoption of subcerebral projection neuron features that are characteristic of later stages of cortical projection neuron development²². Therefore, it is possible that SOX6 and SOX5 both suppress coordinately-regulated controls that promote premature transition into later stages of subtype differentiation. Consistent with this interpretation are the largely redundant roles of both SOX6 and SOX5 in chondroblasts during cartilage development, and in oligodendroglial progenitors in the spinal cord, in preventing the premature transition of these cell types to subsequent stages of development^{32,33}. Given their analogous loss-of-function phenotypes, it is interesting to speculate that SOX6 and SOX5 “separated” in function during the evolution of the increasingly complex neuronal diversity of the telencephalon, and assumed their complementary but distinct roles.

Methods

Mice

Sox6^{+/-} and *Sox5*^{+/-} mice were the generous gift of V. Lefebvre³² (*Sox6* GeneID 20679; *Sox5* GeneID 20678). *GAD67-GFP* (delta-neo) mice were the generous gift of Y. Yanagawa^{28,44}. *Ngn2*^{+/-}/*Ngn1*^{+/-} mice were the generous gift of F. Guillemot⁴. The *Sox6* and *Sox5* transgenic mice are on a pure C57BL/6 background. The *Ngn2/Ngn1* transgenic mice are on a pure CD1 background. The *Sox6/GAD67-GFP* transgenic crosses are a mix between C57BL/6 and Swiss Webster; controls always had the same degree of mixed background. The day of vaginal plug detection was designated as embryonic day 0.5 (E0.5). The day of birth was designated as postnatal day 0 (P0). All mouse studies were approved by the Massachusetts General Hospital IACUC, and were performed in accordance with institutional and federal guidelines.

Immunocytochemistry and *in situ* hybridization

Brains were fixed and stained using standard methods¹⁸. Primary antibodies and dilutions were used as follows: rabbit anti-SOX6, 1:500 (Abcam); goat anti-SOX5, 1:250 (Santa Cruz Biotech); mouse anti-BrdU, 1:500 (Becton Dickinson) (detects IdU); rat anti-BrdU, 1:500 (Accurate) (detects CldU); mouse anti-BrdU, 1:750 (Chemicon); rabbit anti-phospho-histone-H3, 1:200 (Upstate); mouse anti-phospho-histone-H3, 1:400 (Abcam); mouse anti-PCNA, 1:5000 (Sigma); rabbit anti-TBR1, 1:1500, gift of R. Hevner; rabbit anti-TBR1, 1:500 (Abcam); rat anti-CTIP2, 1:1000 (Abcam); mouse anti-Reelin, 1:500 (Chemicon); rabbit anti-GFP, 1:500 (Molecular Probes); mouse anti-PV, 1:500 (Sigma); rat anti-SST, 1:100 (Chemicon); mouse anti-Calb, 1:500 (Chemicon); rabbit anti-Calret, 1:1000 (Chemicon); mouse anti-Calret, 1:400 (Chemicon); rabbit anti-NPY, 1:500 (Immunostar); rabbit anti-VIP, 1:100 (Immunostar); rabbit anti-LHX6, 1:1000, gift of V. Pachnis. Appropriate secondary antibodies were from the Molecular Probes Alexa series. When double immunocytochemistry was performed with two primary antibodies raised in the same

species (only in the case of SOX6 co-localization with NPY and VIP, and NPY co-localization with TBR1 and LHX6): immunocytochemistry for each antibody was performed sequentially using different secondary antibodies; tissue was fixed for 30 minutes in 4% PFA and rinsed in PBS before application of the second primary antibody; and, in instances of minor cross-reactivity, nuclear versus cytoplasmic localization of fluorescence was used to distinguish between the two.

Riboprobes were generated and non-radioactive *in situ* hybridization was performed as previously described¹⁸. The *Sox6* cDNA clone was the gift of V. Lefebvre³². RT-PCR was used to generate the following cDNA clones: *Ngn2*- NM_009718.2 (BGEM); *Mash1*- Riboprobe ID: RP_050927_04_D07 (Allen Brain Atlas); *Olig2*- NM_016967.2 (BGEM); *Pax6*- Riboprobe ID: RP_050927_01_H01 (Allen Brain Atlas); *Cux2*¹⁹; *PlexinD1*¹⁹; *Lhx6*- ID: MTF#274 (Gudmap); *Vglut2*- nucleotides 2477–2933 of NM_080853.

Molecular and mitotic characterization of progenitors

For examination of pallial progenitor phenotype, we performed immunocytochemistry for SOX5 (Fig. 2; n = 5 wildtype and n = 4 *Sox6*^{-/-} at E13.5; n = 4 wildtype and n = 4 *Sox6*^{-/-} at P0), and *in situ* hybridization for *Mash1* (Fig. 3 and Supplementary Fig. 3; n = 3 wildtype, n = 3 *Sox6*^{-/-}, n = 1 *Sox5*^{-/-}, n = 1 *Sox6*^{-/-}/*Sox5*^{-/-} at E13.5; n = 2 wildtype and n = 1 *Ngn2*^{-/-}/*Ngn1*^{-/-} at E14.5; n = 1 wildtype and n = 1 *Sox6*^{-/-} at E17.5), *Sox6* (Fig. 3; n = 2 wildtype and n = 1 *Ngn2*^{-/-}/*Ngn1*^{-/-} at E14.5), *Olig2* (Supplementary Fig. 3; n = 1 wildtype and n = 1 *Sox6*^{-/-} at E13.5) and *Pax6* (Supplementary Fig. 3; n = 1 wildtype and n = 1 *Sox6*^{-/-} at E13.5). For examination of subpallial progenitor phenotype, we performed *in situ* hybridization for *Sox6* (Fig. 2; n = 3 wildtype and n = 2 *Sox6*^{-/-} at E13.5; n = 3 wildtype and n = 3 *Sox6*^{-/-} at P0), and *Ngn2* (Fig. 3 and Supplementary Fig. 3; n = 3 wildtype, n = 2 *Sox6*^{-/-}, n = 1 *Sox5*^{-/-}, n = 1 *Sox6*^{-/-}/*Sox5*^{-/-} at E13.5; n = 1 wildtype and n = 1 *Sox6*^{-/-} at E17.5).

For BrdU birthdating and phospho-histone H3 quantification, timed pregnant females received a single intraperitoneal injection of BrdU (50mg/kg) at E13.5 (pallial progenitor analysis) or E14.5 (subpallial progenitor analysis in Supplementary Fig. 2). Embryos were collected one hour later, and processed for BrdU immunocytochemistry¹⁹. For pallial progenitor quantification, four anatomically matched cortical sections from each mouse were selected (n = 3 wildtype, n = 3 *Sox6*^{-/-}), BrdU and phospho-histone H3 immunocytochemistry were performed (two hours of 2N HCl treatment preceded BrdU immunocytochemistry), fluorescent images were obtained, and two anatomically matched areas (130 μm × 200 μm) from each hemisphere of each section (one medial, one lateral), were selected for blinded quantification of BrdU positivity (defined *a priori* as having strong and homogenous nuclear labeling) and phospho-histone H3 positivity by two independent investigators. Normal distribution was confirmed, and the unpaired, two-tailed t test was used for statistical analysis.

Microarray Analysis

Each embryo of four E13.5 litters (generated by mating male and female *Sox6*^{+/-} mice) was placed in cold HBSS, the pallium was microdissected and immediately preserved in

RNA later (Ambion), and remaining embryo tissue was subsequently genotyped. RNA extraction, quality assessment, and amplification followed previously reported methods¹⁸. Briefly, to ensure biological significance and reproducibility, biological replicate RNA samples from four wildtype and four *Sox6*^{-/-} embryos were extracted using the StrataPrep Total RNA Mini Prep Kit (Stratagene), and RNA was quantified using a NanoDrop (Thermo Fisher Scientific), and quality was assessed with a Nanochip in a Bioanalyzer (Agilent Technologies). RNA was amplified via two rounds of *in vitro* transcription and biotinylated using a BioArray HighYield RNA Transcript Labeling Kit (Enzo), yielding approximately 20–50 µg of labeled cRNA for hybridization¹⁸, and the quality of the amplified RNA was assessed with a Nanochip in a Bioanalyzer before hybridization on Affymetrix 430.2 GeneChips.

Homotypic (biological replicates) and heterotypic comparisons (wildtype vs. *Sox6*^{-/-}) were performed using Rosetta Resolver software (Rosetta Inpharmatics). Differentially expressed genes with an absolute fold change > 1.8 and a p value < 0.005 were selected for further analysis. To rigorously ensure statistical significance of identified candidate genes, data were normalized via three additional independent methods (RMA, gcRMA, and MAS (Affymetrix)) in Bioconductor, and significance of candidate genes were cross-referenced with the Rosetta Resolver normalized dataset. Additional cross-referencing was performed with genes identified as significant with a Significance Analysis of Microarrays (SAM) approach using an absolute fold change > 1.8 and d value of 0.772 for gcRMA normalized data and a d value of 0.35 for RMA normalized data. Biological relevance of candidate genes was assessed in an integrated gene analysis platform developed in our laboratory (Jabaudon, et al., unpublished data), using online *in situ* hybridization, gene ontology, protein function, and literature databases to individually assess expression and function of each gene. Statistically significant genes with normally segregated pallial or subpallial expression during development were identified (Supplementary Table 1).

Mis-expression of SOX6 and SOX5 via Electroporation

For control experiments, a vector containing *IRES-EGFP* under the control of a constitutively active CMV/β-actin promoter was used¹⁹ (a generous gift of C. Lois). *Sox6* and *Sox5*²² were cloned upstream of *IRES-EGFP* for mis-expression. 750 nl of purified DNA (1.0 µg/µl) mixed with 0.005% Fast Green (for visualization) was injected *in utero* into the lateral ventricle of CD1 embryos at E12.5 under ultrasound guidance (Vevo 770, VisualSonics) and electroporated into the subpallial (*Sox6*) or pallial (*Sox5*) ventricular zone, as described^{19,22}. Embryos were analyzed at E16.5 (n = 3 subpallial control, n = 3 subpallial *Sox6*; n = 3 pallial control; n = 3 pallial *Sox5*; multiple independent litters were examined in each condition).

Interneuron Quantification

For quantification of the tangential distance between the leading edges of the MZ and IZ/SVZ interneuron tangential migratory streams at E13.5, anatomically matched sections were selected (n = 3 wildtype/*GAD67-GFP*^{+/-}, n = 3 *Sox6*^{-/-}/*GAD67-GFP*^{+/-}; 10–12 hemispheres per mouse, spanning the rostro-caudal extent of the telencephalon), and GFP immunocytochemistry was performed. The distance was measured in µm between the

position of the soma of the leading neuron of the MZ stream, radially projected to the pial surface, and the corresponding position of the soma of the leading neuron in the IZ/SVZ stream, radially projected to the pial surface, determined by drawing imaginary lines radially from the MZ and IZ/SVZ streams perpendicular to the surface of the brain (Supplementary Fig. 5a).

For quantification of interneuron number at E13.5, anatomically matched sections were selected ($n = 3$ *Sox6*^{+/+}/*GAD67-GFP*^{+/+}, $n = 3$ *Sox6*^{-/-}/*GAD67-GFP*^{+/+}, 10–12 hemispheres per mouse spanning the rostro-caudal extent of the telencephalon), GFP immunocytochemistry was performed, and Grid Confocal (Improvision) images were obtained of a single plane of GFP⁺ neurons. Digital boxes of fixed area (MZ stream: 85 $\mu\text{m} \times 175 \mu\text{m}$; IZ/SVZ stream: 115 $\mu\text{m} \times 175 \mu\text{m}$) were superimposed at predetermined anatomical landmarks at the base, middle, and leading edge of each migratory stream of each hemisphere, and GFP⁺ neurons were quantified (Supplementary Fig. 5b).

For P0 quantification, anatomically matched sections were selected ($n = 3$ wildtype, $n = 3$ *Sox6*^{-/-}; 10–12 hemispheres per mouse spanning the rostro-caudal extent of the telencephalon); GFP immunocytochemistry was performed; digital boxes of fixed width were equally divided into four bins (see Fig. 5a), superimposed on the cortices adjacent to the PSB of each hemisphere, and height was adjusted to extend from the bottom of layer VI to directly under the MZ (at P0 the MZ is still very interneuron dense, and was, therefore, not included in the quantification). GFP⁺ neurons were quantified, and density values were calculated based on the area of the box in each image; densities are expressed as neurons/ mm^2 . Laminar distributions were determined by dividing the proportion of neurons in each bin by the total number of neurons in all bins.

For P14 quantification, anatomically matched sections were selected ($n = 3$ wildtype, $n = 3$ *Sox6*^{-/-}; 8–12 hemispheres per mouse spanning the rostro-caudal extent of the telencephalon); SOX6, GFP, PV, SST, NPY ($n = 6$ wildtype, $n = 6$ *Sox6*^{-/-}), VIP ($n = 4$ wildtype, $n = 4$ *Sox6*^{-/-}), Calret, Calb, and LHX6 immunocytochemistry was performed; digital boxes of fixed width were equally divided into four bins (see Fig. 5b), superimposed on the cortices adjacent to the PSB of each hemisphere, and height was adjusted to extend from the top of the white matter to the cortical surface. The percentages of wildtype interneurons that express SOX6 (Fig. 6b) were calculated from the total numbers in all four bins. Density values and laminar distributions in wildtype and *Sox6*^{-/-} were calculated as above. Quantification (Fig. 6d) is represented as the percent of neuron density in *Sox6*^{-/-} cortex compared to WT.

For IdU and CldU interneuron birthdating, equimolar delivery of IdU (57.5 mg/kg) at E11.5 and CldU (42.5 mg/kg) at E15.5 was performed⁴⁷. Mice were perfused at P14, genotyped, and brains were processed for immunocytochemistry. Anatomically matched sections were selected; IdU, CldU, PV, SST, and NPY immunocytochemistry was performed (IdU and PV, IdU and NPY: $n = 2$ wildtype, $n = 3$ *Sox6*^{-/-}; IdU and SST, CldU and PV, CldU and SST, CldU and NPY: $n = 2$ wildtype, $n = 2$ *Sox6*^{-/-}; 7–8 hemispheres per mouse spanning the rostro-caudal extent of the telencephalon); digital boxes of fixed width were superimposed on the cortices adjacent to the PSB, and height was adjusted to extend from

the top of the white matter to the cortical surface. Interneurons co-expressing SST, PV, or NPY, and either IdU or CldU (defined *a priori* as having strong and homogenous nuclear labeling) were quantified (co-labeling defined as clear nuclear label surrounded by cytoplasmic PV, SST, or NPY label (Fig. 7a)), and density values were calculated based on the area of the box in each image. Quantification (Fig. 7b) is represented as the percent of neuron density in *Sox6*^{-/-} cortex compared to WT.

All quantification was performed on 50 μm vibratome sections using well-established modified stereological methods, beginning at the rostral limit of the corpus callosum and continuing caudally, skipping 4 sections between samples, so that no cell could be double-counted in an adjacent section. We used strict *a priori* criteria whereby the entire soma of a cell needs to be present to be counted, effectively accomplished by counting with high numerical aperture optics within the central approximately 30 μm of the thick 50 μm sections, avoiding cut neurons present in the top or bottom approximately 10 μm of each section. All quantifications were blinded, normal distribution was confirmed, and the unpaired, two-tailed t test was used for statistical analysis; Welch correction was performed in the rare instances when the standard deviations of the two groups varied significantly. All results are expressed as the mean \pm SEM.

Microscopy and image analysis

Tissue sections were viewed on a Nikon E1000 microscope equipped with an X-Cite 120 illuminator (EXFO), and images were collected and analyzed with Volocity image analysis software (Improvision; Version 4.0.1). Images were optimized for size, color, and contrast using Photoshop 7.0. Single plane fluorescence images for E13.5 interneuron quantification were obtained using the Volocity Grid Confocal microscopy system (Improvision); images were collected at the approximate midpoint between the top and bottom planes of focus.

Supplementary Material

Refer to Web version on PubMed Central for supplementary material.

Acknowledgments

This work was partially supported by grants from the National Institutes of Health (NS49553 and NS45523; additional infrastructure supported by NS41590), the Travis Roy Foundation, the Spastic Paraplegia Foundation, the Massachusetts Spinal Cord Injury research program, and the Harvard Stem Cell Institute to J.D.M., and by the Jane and Lee Seidman Fund for CNS Research, and the Emily and Robert Pearlstein Fund for Nervous System Repair. E.A. was partially supported by NIH individual predoctoral NRSA fellowship F31 NS060421. D.J. was partially supported by fellowships from the Swiss National Science Foundation and the Holcim Foundation. R.F. was partially supported by a National Science Foundation Graduate Research Fellowship. We thank K. Billmers, A. Palmer, L. Pasquina, K. Quinn, D. Schuback, E. Sievert, A. Wheeler, and T. Yamamoto for superb technical assistance; Dr. G. Fishell, R. Batista-Brito, Drs. G. Miyoshi, P. Arlotta, B. Molyneaux, H. Padmanabhan, F. Guillemot, Q. Ma, C. Cepko, and L. Goodrich for helpful discussions and input; Dr. U. Berger for technical assistance with *in situ* hybridization; Drs. C. Lois, R. Hevner, V. Lefebvre, F. Guillemot, V. Pachnis, and Y. Yanagawa for generous sharing of mice, antibodies, and reagents; and current and past members of our laboratory for helpful suggestions.

References

1. Schuurmans C, Guillemot F. Molecular mechanisms underlying cell fate specification in the developing telencephalon. *Curr Opin Neurobiol.* 2002; 12:26–34. [PubMed: 11861161]

2. Wonders CP, Anderson SA. The origin and specification of cortical interneurons. *Nat Rev Neurosci.* 2006; 7:687–696. [PubMed: 16883309]
3. Molyneaux BJ, Arlotta P, Menezes JR, Macklis JD. Neuronal subtype specification in the cerebral cortex. *Nat Rev Neurosci.* 2007; 8:427–437. [PubMed: 17514196]
4. Fode C, et al. A role for neural determination genes in specifying the dorsoventral identity of telencephalic neurons. *Genes Dev.* 2000; 14:67–80. [PubMed: 10640277]
5. Parras CM, et al. Divergent functions of the proneural genes *Mash1* and *Ngn2* in the specification of neuronal subtype identity. *Genes Dev.* 2002; 16:324–338. [PubMed: 11825874]
6. Butt SJ, et al. The temporal and spatial origins of cortical interneurons predict their physiological subtype. *Neuron.* 2005; 48:591–604. [PubMed: 16301176]
7. Miyoshi G, Butt SJ, Takebayashi H, Fishell G. Physiologically distinct temporal cohorts of cortical interneurons arise from telencephalic *Olig2*-expressing precursors. *J Neurosci.* 2007; 27:7786–7798. [PubMed: 17634372]
8. Flames N, et al. Delineation of multiple subpallial progenitor domains by the combinatorial expression of transcriptional codes. *J Neurosci.* 2007; 27:9682–9695. [PubMed: 17804629]
9. Wonders CP, et al. A spatial bias for the origins of interneuron subgroups within the medial ganglionic eminence. *Dev Biol.* 2008; 314:127–136. [PubMed: 18155689]
10. Fogarty M, et al. Spatial genetic patterning of the embryonic neuroepithelium generates GABAergic interneuron diversity in the adult cortex. *J Neurosci.* 2007; 27:10935–10946. [PubMed: 17928435]
11. Ascoli GA, et al. Petilla terminology: nomenclature of features of GABAergic interneurons of the cerebral cortex. *Nat Rev Neurosci.* 2008; 9:557–568. [PubMed: 18568015]
12. Flames N, Marin O. Developmental mechanisms underlying the generation of cortical interneuron diversity. *Neuron.* 2005; 46:377–381. [PubMed: 15882635]
13. Corbin JG, Nery S, Fishell G. Telencephalic cells take a tangent: non-radial migration in the mammalian forebrain. *Nat Neurosci.* 2001; 4(Suppl):1177–1182. [PubMed: 11687827]
14. Levitt P, Eagleson KL, Powell EM. Regulation of neocortical interneuron development and the implications for neurodevelopmental disorders. *Trends Neurosci.* 2004; 27:400–406. [PubMed: 15219739]
15. Armijo JA, Valdizan EM, De Las Cuevas I, Cuadrado A. Advances in the pathophysiology of epileptogenesis: molecular aspects. *Rev Neurol.* 2002; 34:409–429. [PubMed: 12040510]
16. Rubenstein JL, Merzenich MM. Model of autism: increased ratio of excitation/inhibition in key neural systems. *Genes Brain Behav.* 2003; 2:255–267. [PubMed: 14606691]
17. Lewis DA. GABAergic local circuit neurons and prefrontal cortical dysfunction in schizophrenia. *Brain Res Brain Res Rev.* 2000; 31:270–276. [PubMed: 10719153]
18. Arlotta P, et al. Neuronal subtype-specific genes that control corticospinal motor neuron development in vivo. *Neuron.* 2005; 45:207–221. [PubMed: 15664173]
19. Molyneaux BJ, Arlotta P, Hirata T, Hibi M, Macklis JD. *Fezl* is required for the birth and specification of corticospinal motor neurons. *Neuron.* 2005; 47:817–831. [PubMed: 16157277]
20. Chen B, Schaevitz LR, McConnell SK. *Fezl* regulates the differentiation and axon targeting of layer 5 subcortical projection neurons in cerebral cortex. *Proc Natl Acad Sci U S A.* 2005; 102:17184–17189. [PubMed: 16284245]
21. Chen JG, Rasin MR, Kwan KY, Sestan N. *Zfp312* is required for subcortical axonal projections and dendritic morphology of deep-layer pyramidal neurons of the cerebral cortex. *Proc Natl Acad Sci U S A.* 2005; 102:17792–17797. [PubMed: 16314561]
22. Lai T, et al. *SOX5* controls the sequential generation of distinct corticofugal neuron subtypes. *Neuron.* 2008; 57:232–247. [PubMed: 18215621]
23. Alcamo EA, et al. *Satb2* regulates callosal projection neuron identity in the developing cerebral cortex. *Neuron.* 2008; 57:364–377. [PubMed: 18255030]
24. Britanova O, et al. *Satb2* is a postmitotic determinant for upper-layer neuron specification in the neocortex. *Neuron.* 2008; 57:378–392. [PubMed: 18255031]
25. Joshi PS, et al. *Bhlhb5* regulates the postmitotic acquisition of area identities in layers II–V of the developing neocortex. *Neuron.* 2008; 60:258–272. [PubMed: 18957218]

26. Kwan KY, et al. SOX5 postmitotically regulates migration, postmigratory differentiation, and projections of subplate and deep-layer neocortical neurons. *Proc Natl Acad Sci U S A*. 2008; 105:16021–16026. [PubMed: 18840685]
27. Cobos I, et al. Mice lacking *Dlx1* show subtype-specific loss of interneurons, reduced inhibition and epilepsy. *Nat Neurosci*. 2005; 8:1059–1068. [PubMed: 16007083]
28. Liodis P, et al. *Lhx6* activity is required for the normal migration and specification of cortical interneuron subtypes. *J Neurosci*. 2007; 27:3078–3089. [PubMed: 17376969]
29. Zhao Y, et al. Distinct molecular pathways for development of telencephalic interneuron subtypes revealed through analysis of *Lhx6* mutants. *J Comp Neurol*. 2008; 510:79–99. [PubMed: 18613121]
30. Du T, Xu Q, Ocbina PJ, Anderson SA. *NKX2.1* specifies cortical interneuron fate by activating *Lhx6*. *Development*. 2008
31. Butt SJ, et al. The requirement of *Nkx2-1* in the temporal specification of cortical interneuron subtypes. *Neuron*. 2008; 59:722–732. [PubMed: 18786356]
32. Smits P, et al. The transcription factors *L-Sox5* and *Sox6* are essential for cartilage formation. *Dev Cell*. 2001; 1:277–290. [PubMed: 11702786]
33. Stolt CC, et al. *SoxD* proteins influence multiple stages of oligodendrocyte development and modulate *SoxE* protein function. *Dev Cell*. 2006; 11:697–709. [PubMed: 17084361]
34. Wegner M. From head to toes: the multiple facets of *Sox* proteins. *Nucleic Acids Res*. 1999; 27:1409–1420. [PubMed: 10037800]
35. Wegner M, Stolt CC. From stem cells to neurons and glia: a *Soxist's* view of neural development. *Trends Neurosci*. 2005; 28:583–588. [PubMed: 16139372]
36. Connor F, Wright E, Denny P, Koopman P, Ashworth A. The *Sry*-related HMG box-containing gene *Sox6* is expressed in the adult testis and developing nervous system of the mouse. *Nucleic Acids Res*. 1995; 23:3365–3372. [PubMed: 7567444]
37. Narahara M, Yamada A, Hamada-Kanazawa M, Kawai Y, Miyake M. cDNA cloning of the *Sry*-related gene *Sox6* from rat with tissue-specific expression. *Biol Pharm Bull*. 2002; 25:705–709. [PubMed: 12081133]
38. Puelles L, et al. Pallial and subpallial derivatives in the embryonic chick and mouse telencephalon, traced by the expression of the genes *Dlx-2*, *Emx-1*, *Nkx-2.1*, *Pax-6*, and *Tbr-1*. *J Comp Neurol*. 2000; 424:409–438. [PubMed: 10906711]
39. Carney RS, et al. Cell migration along the lateral cortical stream to the developing basal telencephalic limbic system. *J Neurosci*. 2006; 26:11562–11574. [PubMed: 17093077]
40. Ma Q, Sommer L, Cserjesi P, Anderson DJ. *Mash1* and *neurogenin1* expression patterns define complementary domains of neuroepithelium in the developing CNS and are correlated with regions expressing notch ligands. *J Neurosci*. 1997; 17:3644–3652. [PubMed: 9133387]
41. Scardigli R, Baumer N, Gruss P, Guillemot F, Le Roux I. Direct and concentration-dependent regulation of the proneural gene *Neurogenin2* by *Pax6*. *Development*. 2003; 130:3269–3281. [PubMed: 12783797]
42. Britz O, et al. A role for proneural genes in the maturation of cortical progenitor cells. *Cereb Cortex*. 2006; 16(Suppl 1):i138–151. [PubMed: 16766700]
43. Batista-Brito R, Machold R, Klein C, Fishell G. Gene Expression in Cortical Interneuron Precursors is Precursor of their Mature Function. *Cereb Cortex*. 2008
44. Tamamaki N, et al. Green fluorescent protein expression and colocalization with calretinin, parvalbumin, and somatostatin in the *GAD67-GFP* knock-in mouse. *J Comp Neurol*. 2003; 467:60–79. [PubMed: 14574680]
45. Cavanagh ME, Parnavelas JG. Development of somatostatin immunoreactive neurons in the rat occipital cortex: a combined immunocytochemical-autoradiographic study. *J Comp Neurol*. 1988; 268:1–12. [PubMed: 2894382]
46. Cavanagh ME, Parnavelas JG. Development of neuropeptide Y (NPY) immunoreactive neurons in the rat occipital cortex: a combined immunohistochemical-autoradiographic study. *J Comp Neurol*. 1990; 297:553–563. [PubMed: 1974557]
47. Vega CJ, Peterson DA. Stem cell proliferative history in tissue revealed by temporal halogenated thymidine analog discrimination. *Nat Methods*. 2005; 2:167–169. [PubMed: 15782184]

48. Holm PC, et al. Loss- and gain-of-function analyses reveal targets of Pax6 in the developing mouse telencephalon. *Mol Cell Neurosci.* 2007; 34:99–119. [PubMed: 17158062]
49. Molnar Z, Butler AB. The corticostriatal junction: a crucial region for forebrain development and evolution. *Bioessays.* 2002; 24:530–541. [PubMed: 12111736]
50. Nobrega-Pereira S, et al. Postmitotic Nkx2-1 controls the migration of telencephalic interneurons by direct repression of guidance receptors. *Neuron.* 2008; 59:733–745. [PubMed: 18786357]

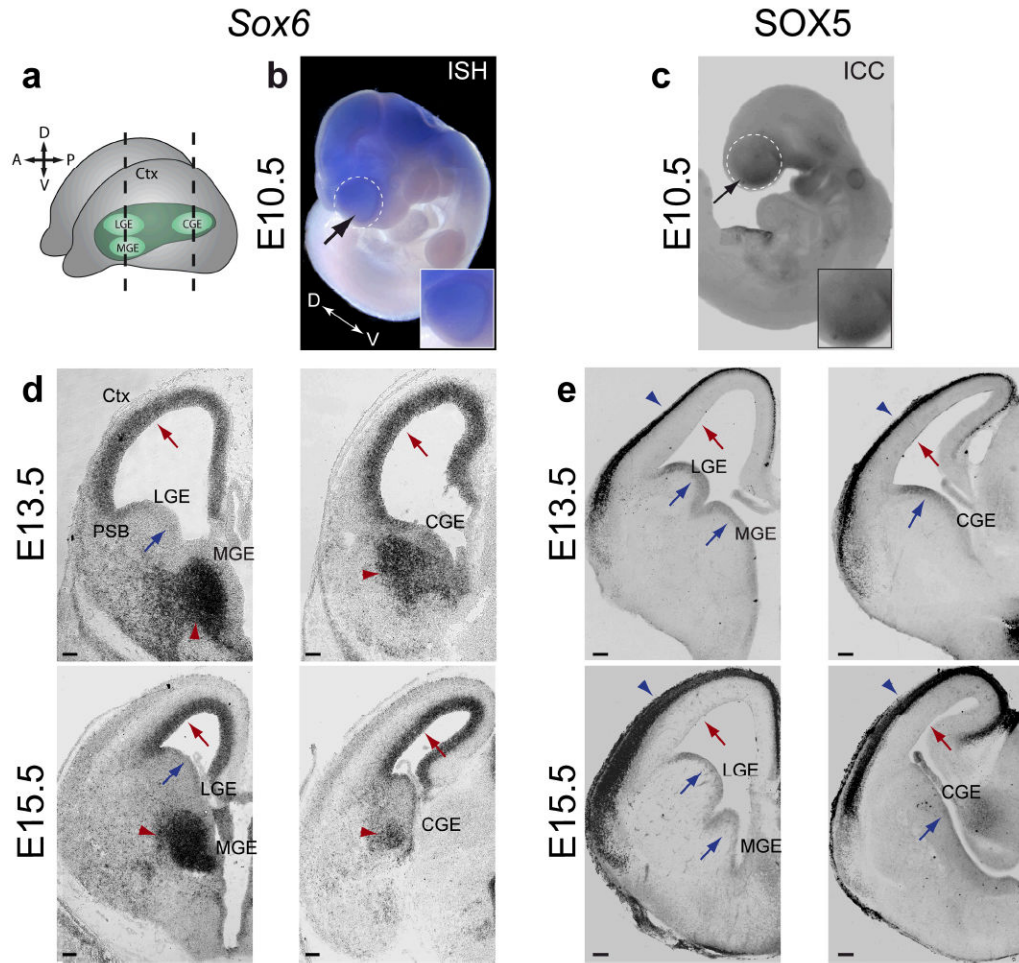


Figure 1. SOX6 and SOX5 are expressed in complementary populations of telencephalic progenitors and neuronal progeny during corticogenesis. **(a)** Schematic illustrating the relative position of the neocortex, LGE, MGE, and CGE in the developing brain. **(b,c)** *Sox6* **(b)**; black arrow) is expressed in a slight dorsal-high ventral-low gradient, and SOX5 **(c)**; black arrow) is expressed in a ventral-high dorsal-low gradient in the telencephalon (white dotted circles) at E10.5, as corticogenesis is beginning. Insets show higher magnification view of the telencephalon. **(d,e)** During corticogenesis, shown here at E13.5 and E15.5, *Sox6* **(d)** is expressed in progenitors of the pallial ventricular zone (VZ) (red arrows) and in postmitotic neurons in the MGE and CGE mantle zones (red arrowheads), but it is not expressed in subpallial VZ progenitors (blue arrows). SOX5 **(e)** is expressed in subpallial VZ progenitors (blue arrows) and postmitotic neurons in the cortical plate (blue arrowheads), but it is not expressed in pallial VZ progenitors (red arrows). **(a)** adapted from¹³. **(b,d)** ISH, *in situ* hybridization; **(c,e)** ICC, immunocytochemistry. Ctx, cortex; PSB, pallial-subpallial boundary; LGE, lateral ganglionic eminence; MGE, medial ganglionic eminence; CGE, caudal ganglionic eminence. Scale bars, **(d,e)**; E13.5) 100 μ m, **(d,e)**; E15.5) 150 μ m.

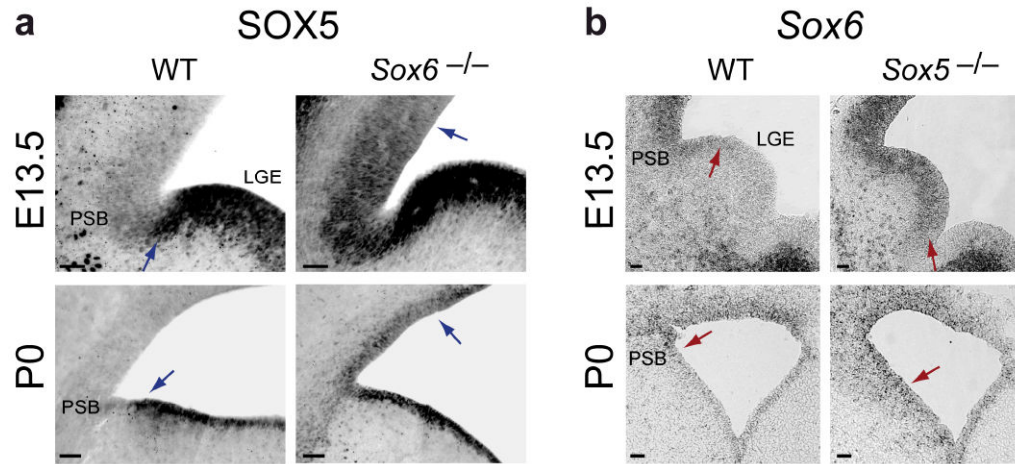
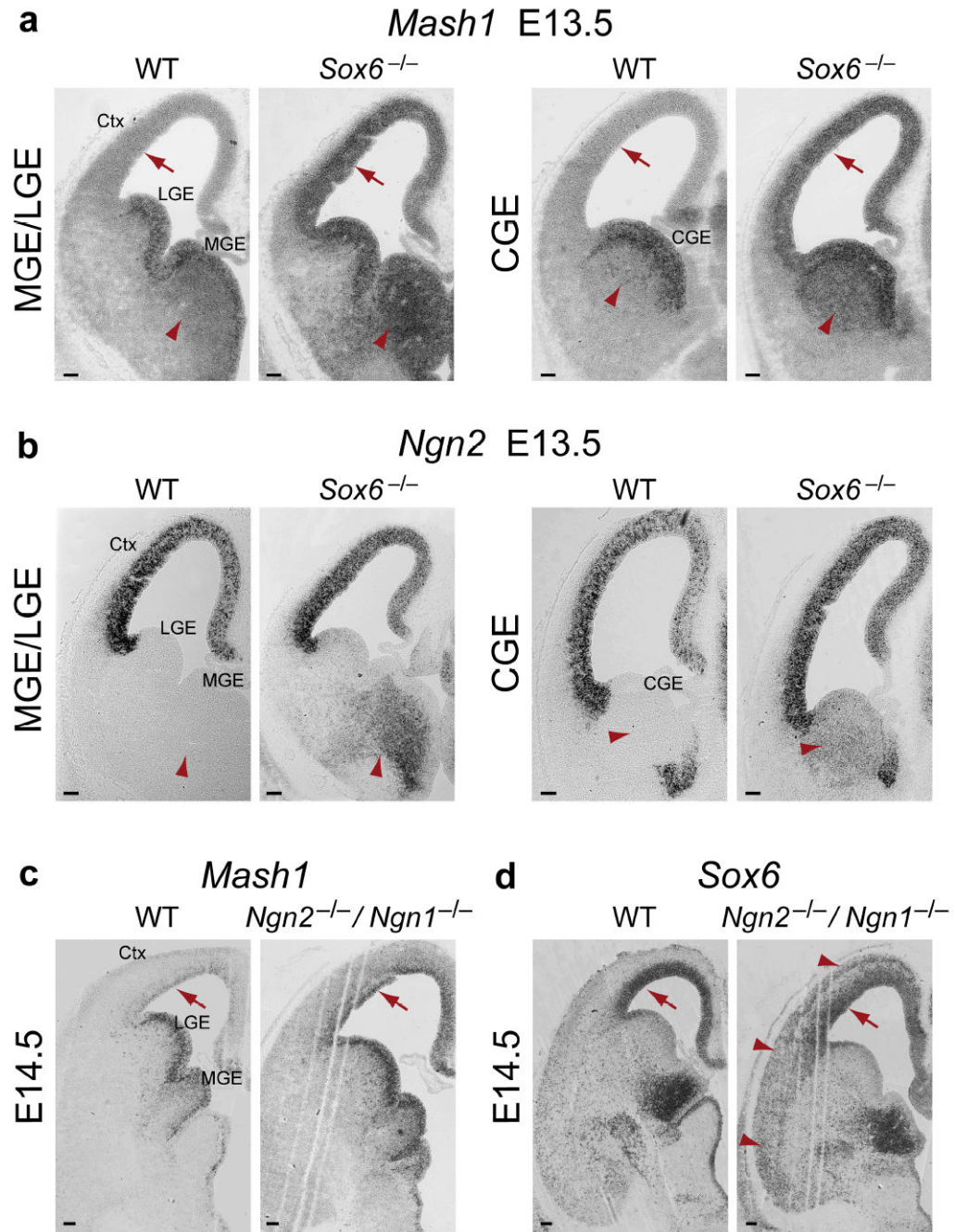


Figure 2.

SOX6 and SOX5 are cross-repressive in pallial and subpallial telencephalic progenitor domains. **(a)** SOX5 expression, which normally extends to the ventral edge of the pallial-subpallial boundary (blue arrows in WT) and is absent from pallial VZ progenitors, shown here at E13.5 and P0, ectopically expands into *Sox6*^{-/-} pallial VZ progenitors (blue arrows in *Sox6*^{-/-}). This SOX5 expansion is most pronounced near the pallial-subpallial boundary (PSB) at E13.5, and extends evenly throughout progenitors of the entire pallial VZ by P0. **(b)** Conversely, *Sox6* expression, which normally extends to the dorsal edge of the PSB (red arrows in WT) and is absent from subpallial progenitors, shown here at E13.5 and P0, ectopically expands into *Sox5*^{-/-} subpallial VZ progenitors (red arrows in *Sox5*^{-/-}). This *Sox6* expansion is most pronounced near the PSB in the LGE at E13.5, and extends evenly throughout progenitors of the entire subpallial VZ by P0. **(a)** immunocytochemistry; **(b)** *in situ* hybridization. WT, wildtype; PSB, pallial-subpallial boundary; LGE, lateral ganglionic eminence. Scale bars, **(a,b)** 50 μ m.

**Figure 3.**

Loss of SOX6 function results in ectopic proneural gene expression in pallial progenitors and subpallial mantle zones. **(a)** *Mash1*, which is normally restricted to subpallial VZ progenitors, and is not expressed by pallial VZ progenitors (red arrows) or by postmitotic neurons in subpallial mantle zones (red arrowheads), is ectopically expressed in *Sox6*^{-/-} pallial VZ progenitors, and is ectopically expressed in the MGE and CGE mantle zones, shown here at E13.5. **(b)** *Ngn2*, which is normally restricted to pallial VZ progenitors, and is not expressed by postmitotic neurons in subpallial mantle zones (red arrowheads), is

ectopically expressed in *Sox6*^{-/-} MGE and CGE mantle zones, shown here at E13.5. **(c)** As previously reported⁴, *Mash1*, which is normally not strongly expressed in pallial VZ progenitors, shown here at E14.5 (red arrows), is ectopically expressed in progenitors of the *Ngn2*^{-/-}/*Ngn1*^{-/-} pallial VZ. **(d)** As in the wildtype, SOX6 continues to be expressed in *Ngn2*^{-/-}/*Ngn1*^{-/-} pallial VZ progenitors (red arrows). SOX6 is ectopically expressed in *Ngn2*^{-/-}/*Ngn1*^{-/-} postmitotic pallium-derived neurons in the cortical plate (red arrowheads), consistent with the ectopic expression of subpallial postmitotic signals in pallium-born neurons in the absence of Ngn2 function, as previously described^{4,5}. **(a-d)** *in situ* hybridization. WT, wildtype; Ctx, cortex; LGE, lateral ganglionic eminence; MGE, medial ganglionic eminence; CGE, caudal ganglionic eminence. Scale bars, **(a-d)** 100 μ m.

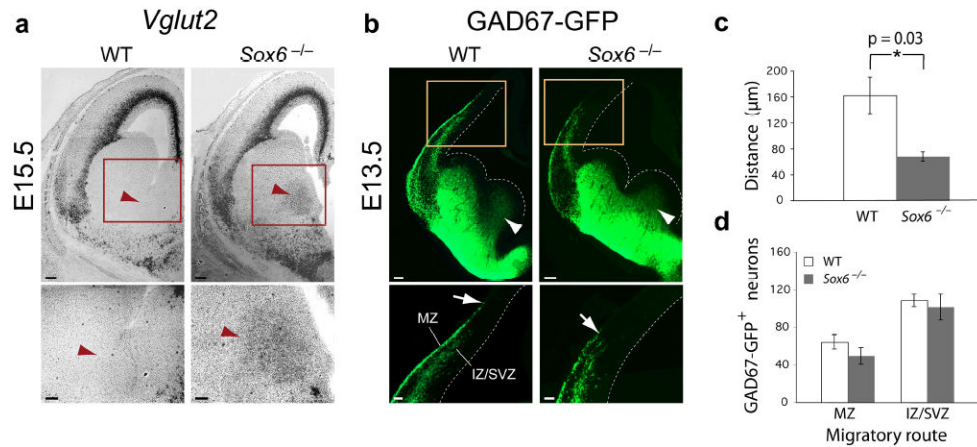
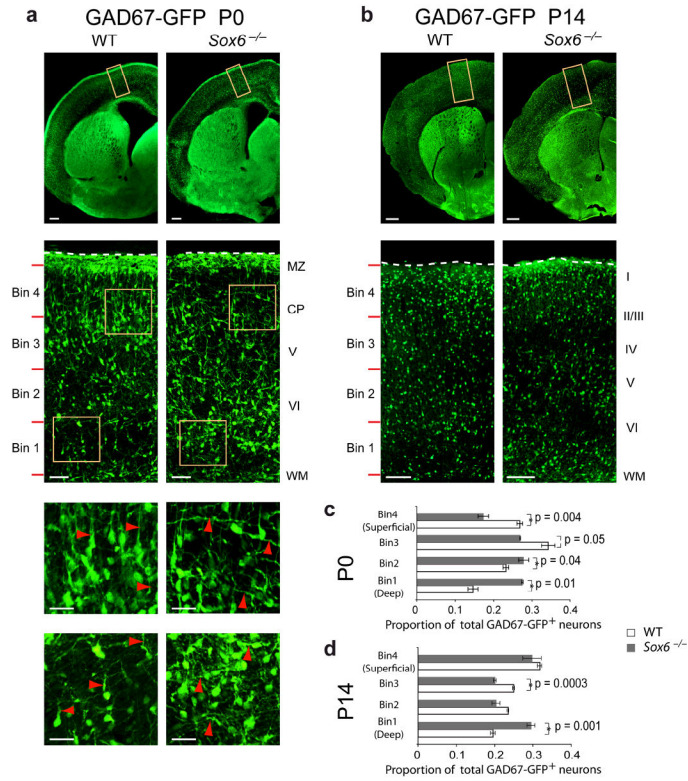


Figure 4.

Loss of SOX6 function results in abnormal early cortical interneuron differentiation, without a change in interneuron number. **(a)** While excitatory neuron-specific *Vglut2* is not normally expressed in neurons born in the subpallium, shown here at E15.5 (red arrowheads), in *Sox6*^{-/-} mice, *Vglut2* is ectopically expressed in the subpallial mantle zone. **(b,c)** GAD67-GFP⁺ neurons are born in both wildtype and *Sox6*^{-/-} MGE (white arrowheads). However, as GABAergic cortical interneurons tangentially migrate into the cortex, the leading edge of the marginal zone (MZ) migratory stream is consistently less advanced in the *Sox6*^{-/-} cortex compared to wildtype (white arrows) (60% reduction in distance; $p = 0.03$ **(c)**). **(d)** There is no difference between wildtype and *Sox6*^{-/-} cortex in the number of migrating cortical interneurons in either the MZ or IZ/SVZ migratory streams. **(a)** *in situ* hybridization; **(b)** immunocytochemistry. WT, wildtype; MZ, marginal zone; IZ, intermediate zone; SVZ, subventricular zone. Dotted lines **(b)** indicate lateral ventricle boundary. Scale bars, **(a)** (low magnification) 150 μm, **(a)** (high magnification, **b**; low magnification) 100 μm, **(b)** (high magnification) 50 μm. Results are expressed as the mean ± SEM.

**Figure 5.**

Loss of SOX6 function disrupts the normal laminar position and morphology of cortical interneurons. Analysis of *GAD67-GFP* mice reveals that, while there are equal numbers of cortical interneurons at P0 (**a**) and P14 (**b**) in WT and *Sox6*^{-/-} cortex, there is a redistribution of interneurons toward deeper cortical layers in *Sox6*^{-/-} cortex compared to WT (**c,d**). Quantification at P0 (**c**) reveals a proportional increase in interneuron density in the deepest bin 1 by 13% ($p = 0.01$) and bin 2 by 5% ($p = 0.04$), and a proportional decrease in more superficial bin 3 by 7% ($p = 0.05$) and bin 4 by 10% ($p = 0.004$). Quantification at P14 (**d**) reveals an increase in interneuron density in the deepest bin 1 by 10% ($p = 0.0001$) and a decrease in the more superficially located bin 3 by 5% ($p = 0.0003$). Red lines (**a,b**) indicate subdivision into 4 bins for quantification (see Methods). Interneurons have abnormal tangential morphology in *Sox6*^{-/-} cortex compared to the radially oriented interneurons in WT cortex (**a**; red arrowheads). (**a,b**) immunocytochemistry. WT, wildtype; MZ, marginal zone; CP, cortical plate; WM, white matter. Dotted lines (**a,b**) indicate pial surface. Scale bars, (**a**; low magnification) 200 μm , (**a**; intermediate magnification) 50 μm , (**a**; high magnification) 25 μm , (**b**; low magnification) 300 μm , (**b**; high magnification) 100 μm . Results are expressed as the mean \pm SEM.

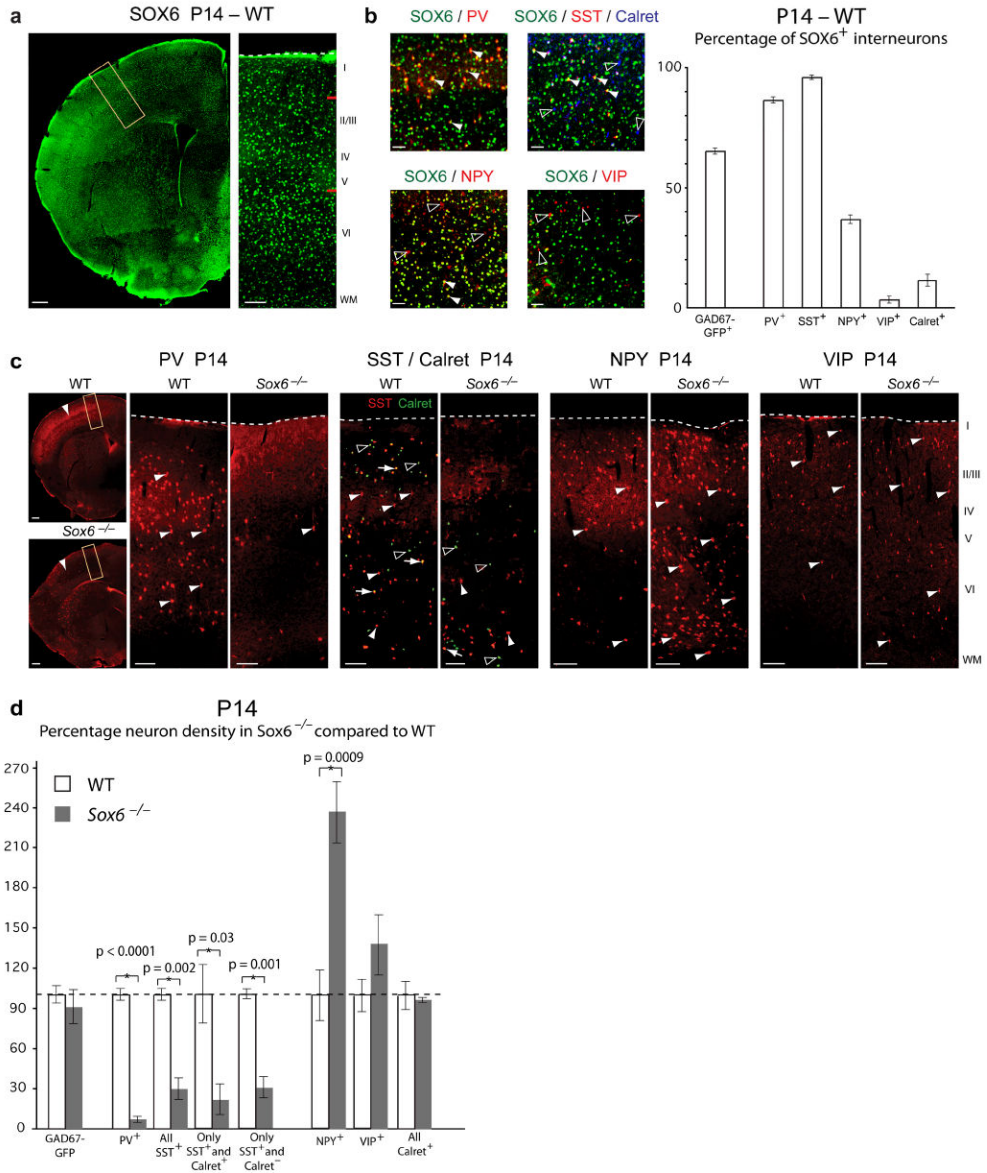
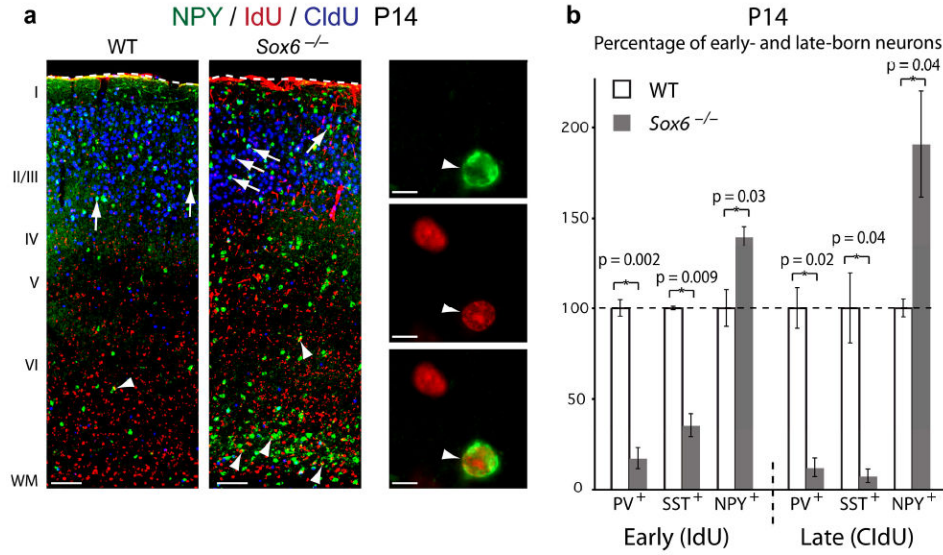
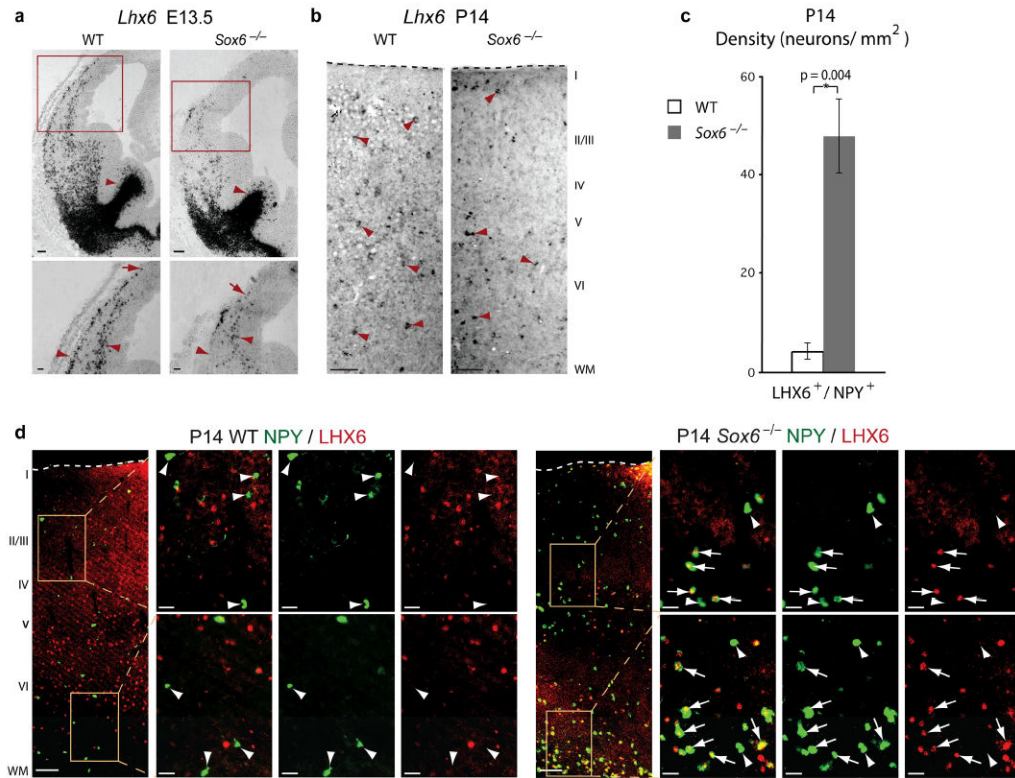


Figure 6. SOX6 is necessary for cortical interneuron subtype development. **(a,b)** At P14, SOX6 is expressed by ~65% of all neocortical GAD67-GFP⁺ interneurons, including essentially all PV⁺ (86%) (white arrowheads), SST⁺ (96%) (white arrowheads), SST⁺/Calret⁺ (83%), and SST⁺/Calret⁻ (95%) interneurons; over 1/3 of all NPY⁺ interneurons (37%) (white arrowheads; open arrowheads indicate NPY⁺/SOX6⁻ interneurons); essentially no VIP⁺ interneurons (3%) (open arrowheads indicate VIP⁺/SOX6⁻ interneurons); and very few of all Calret⁺ interneurons (11%) (open arrowheads indicate Calret⁺/SOX6⁻ interneurons). Red lines in **(a)** indicate approximate regions of magnification in **(b)**. **(c,d)** At P14, PV⁺ cortical interneuron numbers (white arrowheads) are dramatically diminished in *Sox6*^{-/-} compared to WT cortex (93% reduction; p < 0.0001), as are SST⁺ cortical interneuron numbers (red neurons; white arrowheads) (70% reduction; p = 0.002). There is no change in the number of Calret⁺ interneurons (green neurons; open arrowheads), though the subset of SST⁺/Calret⁺

interneurons (yellow neurons; white arrows) is reduced in number in *Sox6*^{-/-} compared to WT cortex (79% reduction; $p = 0.03$). The subset of SST⁺/Calret⁻ interneurons is also reduced (70% reduction; $p = 0.001$). The number of NPY⁺ cortical interneurons (white arrowheads) is dramatically increased in *Sox6*^{-/-} compared to WT cortex (137% increase; $p = 0.0009$). There is no change in the number of VIP⁺ interneurons (white arrowheads). The positions of the yellow boxes in low magnification panels (**c**) are representative of the neocortical position examined in high magnification panels. Quantification in (**d**) is represented as the percentage of neuron density in *Sox6*^{-/-} compared to WT. (**a-c**) immunocytochemistry. WT, wildtype; WM, white matter. Dotted lines (**a,c**) indicate pial surface. Scale bars, (**a,c**; low magnification) 300 μm , (**a,c**; high magnification) 100 μm , (**b**) 50 μm . Results are expressed as the mean \pm SEM.

**Figure 7.**

Loss of SOX6 function produces an increased number of early- and late-born NPY⁺ cortical interneurons. **(a,b)** Dual birthdating of cortical interneurons using IdU (E11.5) and CldU (E15.5) reveals a dramatic decrease in the number of PV⁺ and SST⁺ early- and late-born interneurons (early PV: 83% decrease; $p = 0.002$; early SST: 65% decrease; $p = 0.009$; late PV: 88% decrease; $p = 0.02$; late SST: 93% decrease; $p = 0.04$ **(b)**), and a large increase in the number of NPY⁺ early- (white arrowheads) and late-born (white arrows) interneurons (early NPY: 40% increase; $p = 0.03$; late NPY: 90% increase; $p = 0.04$ **(b)**). Co-localization was strictly assessed as homogenous, strong nuclear IdU or CldU label surrounded by cytoplasmic PV, SST, or NPY labeling (NPY/IdU co-localization provided as a representative example in **(a)**; white arrowhead). Quantification in **(b)** is represented as the percentage of neuron density in *Sox6*^{-/-} cortex compared to WT. **(a)** immunocytochemistry. WT, wildtype; WM, white matter. Dotted lines **(a)** indicate pial surface. Scale bars, **(a)**; low magnification) 100 μm , **(a)**; high magnification) 10 μm . Results are expressed as the mean \pm SEM.

**Figure 8.**

SOX6 control over MGE-derived cortical interneuron subtype differentiation is population autonomous. **(a)** At E13.5, during early stages of cortical interneuron differentiation, MGE-born interneurons in WT and *Sox6*^{-/-} telencephalon express *Lhx6* (low magnification; red arrowheads), but the development of these neurons is disrupted in *Sox6*^{-/-} mice; as the migratory streams are disorganized compared to WT (high magnification; red arrowheads), and the leading edge of the MZ migratory stream compared to the IZ/SVZ stream is consistently shorter in *Sox6*^{-/-} mice compared to WT (red arrows). **(b)** At P14, a large subset of *Lhx6*⁺ neurons present in the cortex of WT mice have populated the maturing *Sox6*^{-/-} cortex (red arrowheads). **(c,d)** At P14 in WT cortex, the vast majority of LHX6⁺ neurons (99% ± 0.5%) do not express NPY **(d; white arrowheads)**, while in *Sox6*^{-/-} cortex, LHX6⁺ neurons dramatically increase their co-expression of NPY **(d; white arrows)** (~11.5-fold increase; $p = 0.004$ **(c)**), especially in deeper layers (81% ± 5% of co-localization in the two deepest bins; see Fig. 5b for bin placement). Quantification in **(c)** is represented as the density of neurons/mm². **(a,b)** *in situ* hybridization; **(d)** immunocytochemistry. WT, wildtype; WM, white matter. Dotted lines **(b,d)** indicate pial surface. Scale bars, **(a; low magnification, b, d; low magnification)** 100 μm, **(a; high magnification)** 50 μm, **(d; high magnification)** 25 μm. Results are expressed as the mean ± SEM.